Boosting Electric Double Layer Capacitance in Laser-Induced Graphene-Based Supercapacitors

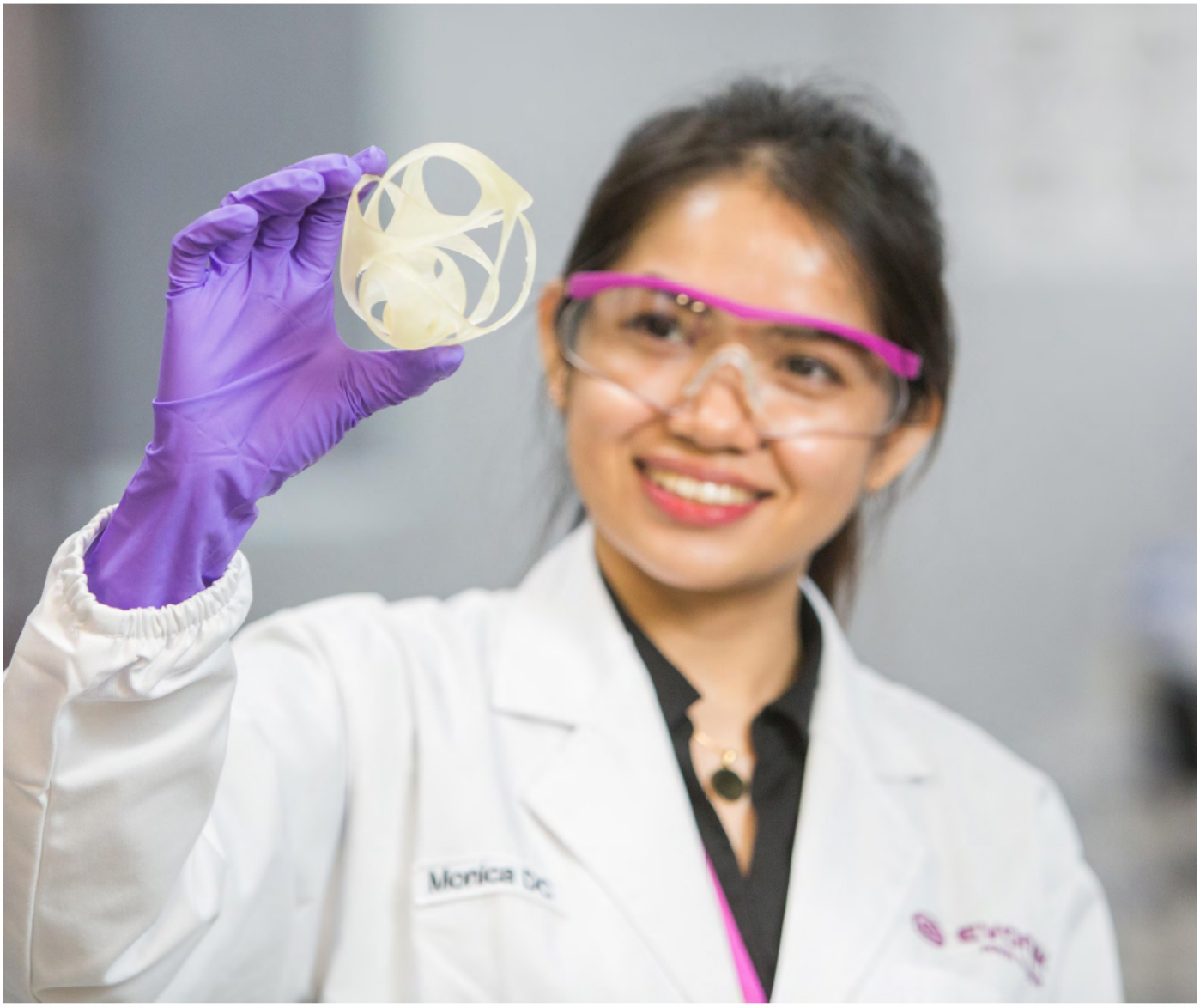

Pushing the boundaries of chemistry? It takes #HumanChemistry

Make your curiosity and talent as a chemist matter to the world with a specialty chemicals leader. Together, we combine cutting-edge science with engineering expertise to create solutions that answer real-world problems. Find out how our approach to technology creates more opportunities for growth, and see what chemistry can do for you at:

evonik.com/career

EVONIK
Leading Beyond Chemistry

ADVANCED SUSTAINABLE SYSTEMS
www.advsustainsys.com

Boosting Electric Double Layer Capacitance in Laser-Induced Graphene-Based Supercapacitors

*Marco Reina, Alberto Scalia, Giorgio Auxilia, Marco Fontana, Federico Bella, Sergio Ferrero, and Andrea Lamberti**

Laser-induced graphene (LIG) is under the spotlight as a promising material for flexible supercapacitors due to its simple processing and flexibility. However, the poor conductivity and the reduced surface area have prompted research to improve its performance, traditionally introducing a pseudocapacitive behavior. Herein an effective yet easy way is presented to dramatically improve the electric double layer capacitance of LIG electrodes for supercapacitor-related applications without the occurrence of redox reactions. The strategy simply relies on the exploitation of an LIG network to trap and interconnect activated carbon (AC) particles. In order to optimize the infiltration of AC into LIG porosities, several strategies are tested, both varying the surface wettability of LIG and acting on the impregnation approach. Overall, the best compromise results in the combination of LIG N-doping by nitric acid incubation with vacuum-assisted infiltration of an AC-slurry, allowing a two-order of magnitude improvement in the specific capacitance up to 20 mF cm^{-2} in device configuration.

1. Introduction

Laser-induced graphene (LIG) is nowadays among the most studied materials for electrical double layer (EDL) microsupercapacitors (μSCs) thanks to the intrinsically simple fabrication approach on polymeric supports, the low cost, and the flexibility of the resulting electrodes.[1–3] It consists of a 3D network of few layer graphene (FLG) walls obtained by a direct laser writing process during which the sp^3 carbon atoms in the polymer are photothermally converted to sp^2 carbon atoms. The gas evolution due to the partial decomposition of the polymer chain acts as bubble-template during the graphitization, resulting in an electrically conductive porous structure suitable for supercapacitors application. Moreover, LIG acts at the same time as current collector and binder-free active material, strongly simplifying the device fabrication process, similarly to other direct-laser written materials.[4]

Apart from the advantages discussed above, the sheet resistance of LIG is higher than that of traditional thin films used as current collectors in μSCs and the active material loading is lower if compared to FLG-based electrodes prepared through more complicated experimental approaches.[5]

For these reasons, three main strategies have been proposed up to now to overcome the limitations cited above, i.e., i) improving the conductivity of LIG acting on the laser writing parameters, ii) doping LIG in order to increase the electrochemical performance, and iii) decorating LIG surface with pseudocapacitive materials to increase the specific capacitance of the electrodes, allowing Faradaic reaction occurrence.

Concerning the first approach, the main parameters investigated in the literature are the laser beam power, the pulse frequency and the scanning speed (variable depending on the laser equipment used for the process). Usually, for microsecond pulsed CO_2 laser source, increasing the laser power (in the 1–6 W range) leads to an improvement of LIG conductivity up to maximum value, then it starts decreasing due to the decomposition of the polymer with subsequent ablation.[6] The frequency increase (typically in the 4–24 kHz range) positively affects the electrical conductivity of LIG, resulting in improved capacitive performance.[7] Finally, the scanning speed can be varied, but its selection must be strongly considered as a function of power and pulse frequency in order to provide a certain dose of impinging energy (a critical fluence of ≈5.5 J cm^{-2} was required to obtain LIG on poly(imide)) to allow photothermal conversion of the polymeric matrix into FLG.[8]

Among the possible doping elements, boron and nitrogen have been investigated by adding boric acid into the polymer matrix before laser writing[9] or by incubating the written LIG electrode into nitric acid,[10] respectively. Both the approaches result in the improvement of the conductivity and

M. Reina, A. Scalia, G. Auxilia, M. Fontana, F. Bella, S. Ferrero, A. Lamberti
Politecnico di Torino
Dipartimento di Scienza Applicata e Tecnologia (DISAT)
Corso Duca Degli Abruzzi
24, Torino 10129, Italy
E-mail: andrea.lamberti@polito.it

M. Reina, M. Fontana, A. Lamberti
Istituto Italiano di Tecnologia
Center for Sustainable Future Technologies
Corso Trento
21, Torino 10129, Italy

The ORCID identification number(s) for the author(s) of this article can be found under https://doi.org/10.1002/adsu.202100228.

DOI: 10.1002/adsu.202100228

electrochemical response of LIG. Moreover, N-doping was demonstrated to induced higher hydrophilicity in the graphitic network, permitting higher infiltration of water-based electrolytes.

With reference to the latter strategy, several pseudocapacitive materials allowing Faradaic reaction occurrence have been published. Tour and coworkers electrodeposited MnO_2, FEOOH, and poly(aniline) on LIG, with an astonishing enhancement of the specific capacitance up to 1 F cm^{-2} and with a capacitance retention of about 80% after 2000 cycles.[11]

Clerici et al. coupled LIG electrodes with MoS_2 nanoflakes, exploiting an in situ decoration by spin-coating MoS_2 flakes on poly(imide) foil before laser writing. The obtained LIG results decorated by MoS_2 flakes, leading to an improvement of about four times in terms of specific capacitance.[12]

Zhang et al. infiltrated ZnP mesoporous flakes in the LIG porosity, leading to an increase of the hydrophilicity and the introduction of pseudocapacitance in the carbon-based electrodes.[13]

Finally, Song et al. deposited a film of poly(3,4-ethylenedioxythiophene) by drop casting method after a nitric acid treatment, observing a marked improvement in electrochemical performance of the electrodes.[10]

LIG decoration with other kinds of nanoparticles was also investigated in sectors different than that of energy storage, such as chemical and physical sensing, in order to induce multifunctional properties to the conductive path or to reduce the electrical resistance.[14–17]

Nevertheless, no attempts have been proposed up to now to increase the active material loading in order to exploiting only EDL storage mechanism. Herein, we report for the first time the decoration of LIG with activated carbon (AC) particles by a carefully designed approach (see **Figure 1**).

2. Results and Discussion

The effectiveness of the laser writing procedure on the polyimide foil has been investigated in previous publications of the same authors' group. Indeed, Raman, X-ray photoelectron spectroscopy, and transmission electron microscopy analysis demonstrate the FLG nature of LIG.[7,12,18–20]

Concerning the possibility to increase the specific electric double layer capacitor (EDLC) performance of LIG, first of all the infiltration step was analyzed (see Figure 1), since a template can be filled following different strategies, namely dip coating, drop casting, or vacuum infiltration. All of them were implemented exploiting a dimethyl sulfoxide (DMSO)-based AC slurry and the results were compared with those of bare LIG electrode.

The first approach simply consisted on vertically dipping LIG electrode (or device) into a diluted dispersion containing AC : carbon black (CB, CC) : poly(vinylidene fluoride) (PVDF) with the proportion (by weight) of 85:10:5.

The second approach consisted on depositing few droplets of the diluted solution aforementioned onto the LIG portion, letting DMSO solvent to evaporate.

The last approach was carried out immersing the LIG electrode (or device) into the diluted dispersion based on AC, CC, and PVDF, simultaneously applying vacuum in the area of the sample by means of a funnel connected to a membrane-based pump.

Figure 2a shows the cyclic voltammetry (CV) traces of AC nanoparticles trapped LIG and bare LIG, performed in a three-electrode configuration with a scan rate of 10 mV s^{-1}. The potential window (0–0.5 V) was chosen in order to be sure that the electrode could work under optimal conditions, showing a

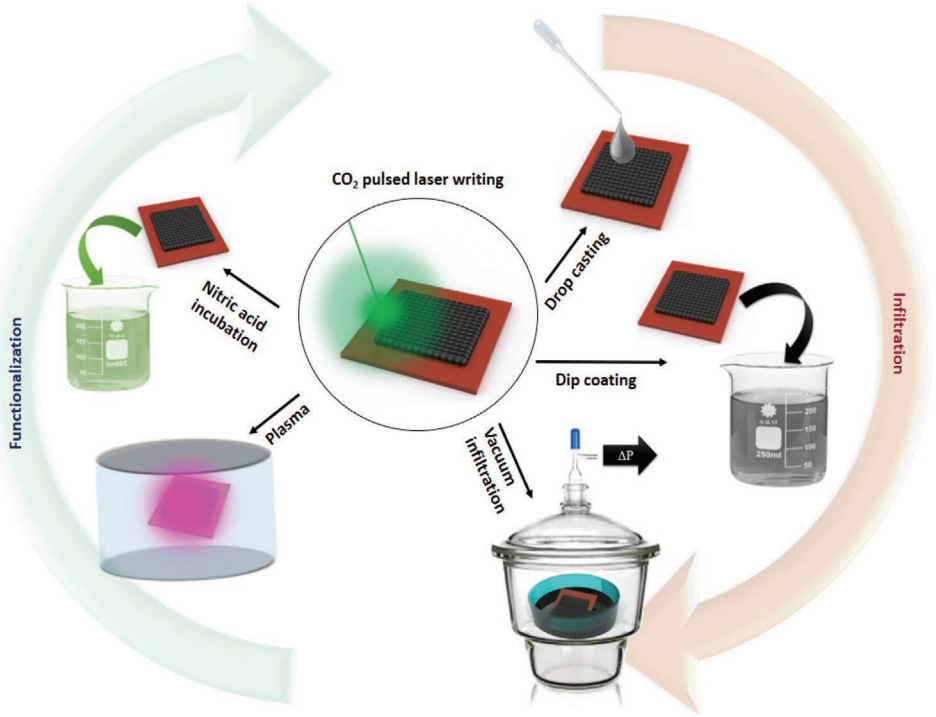

Figure 1. Scheme of the sample processing after laser writing using different functionalizations (on the left: N-doping by nitric acid incubation and plasma treatment) and infiltration approaches (on the right: drop casting, dip coating, and vacuum infiltration).

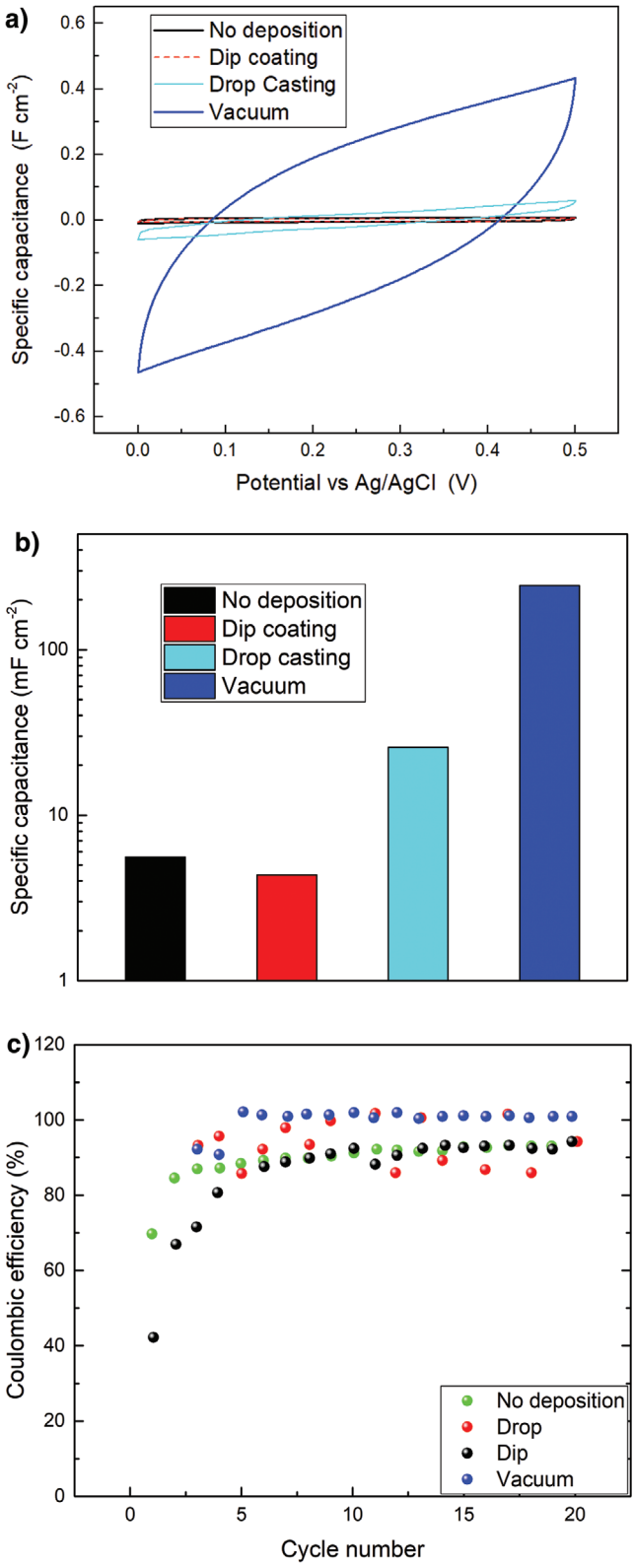

Figure 2. a) CVs carried out in a three-electrode configuration of samples prepared by dip coating, drop casting, and vacuum deposition methods, compared with a bare sample. b) Specific capacitance of the same electrodes, evaluated by CV measurements. c) Coulombic efficiency values for cells assembled with electrodes subjected to different treatments.

Coulombic efficiency higher than 95% (see Figure S1, Supporting Information). Evidently, the vacuum infiltration resulted to be the most effective solution in order to infiltrate AC particles into LIG porosity (surface area and pore volume analysis was discussed in the Supporting Information), thus increasing the specific capacitance of the active material. All the laser writing parameters for LIG electrodes preparation were kept constant among the four samples analyzed, and a nondecorated LIG sample was added to the plot for comparison. Moreover, we performed electrical measurement of the electrodes before and after the AC vacuum infiltration. The measurements have been conducted in order to evaluate the sheet resistance, i.e., the main figure of merit usually encountered in all the literature works related to LIG. The measure has been carried out by fabricating an LIG-based Van Der Pauw's cross (see Figure S5, Supporting Information) and exploiting the Van der Pauw's evaluation method. The results indicate a reduction of the sheet resistance from 37 to 30 Ω square^{-1}.

In Figure 2b, the values of specific capacitance are reported along a logarithmic *y*-axis, thus testifying that the vacuum process infiltration led to an outstanding two-order of magnitude increment with respect to bare LIG.

As shown in Figure 2c, the efficiency was very high for all the tested samples, but the C_{sp} was two orders of magnitude higher in vacuum infiltrated samples with respect to dip-coating and nontreated samples, and one order of magnitude larger than drop-casted electrode. Moreover, a study of the amount of active material deposited with respect to vacuum infiltration time has been carried out. Then, the capacitive performances have been evaluated for different quantities of active material, obtaining almost a direct relationship between the increase of capacitance and the material loading up to 120 s of incubation (see Figure S6, Supporting Information). After that, the capacitance starts to saturate in material loading when further increasing the time up to 300 s. The possible reason relies on the fact that, after a certain time of incubation, all the macroporosities of the LIG network are filled with AC particles. Even if some other AC particles can start accumulating on top of LIG, they are removed after the rinsing procedure when the electrode is extracted from the solution.

Considering the advantage of this last approach with respect to drop casting and dip coating, we coherently decided to go ahead with the vacuum infiltration method to fabricate LIG-based supercapacitors.

Since LIG obtained with the parameters described in the experimental section is normally hydrophobic, different ways to increase its wettability are studied, since both the active material slurry and the electrolyte are based on a polar solvent. The two selected methods involve dry and wet approaches, i.e., plasma and nitric acid treatments. To the best of our knowledge, this is the first time that a plasma treatment is used on LIG to tune its wettability, while some reports can be found about the activation using nitric acid.[10,21] The nitric acid treatment consisted of 30 s dipping in a 69% nitric acid commercial solution, followed by rinsing in distilled water for 1 min. After letting the sample dry in oven to remove all the excess of water, the LIG was infiltrated with AC slurry. Conversely, the argon plasma treatment was performed in a sputtering

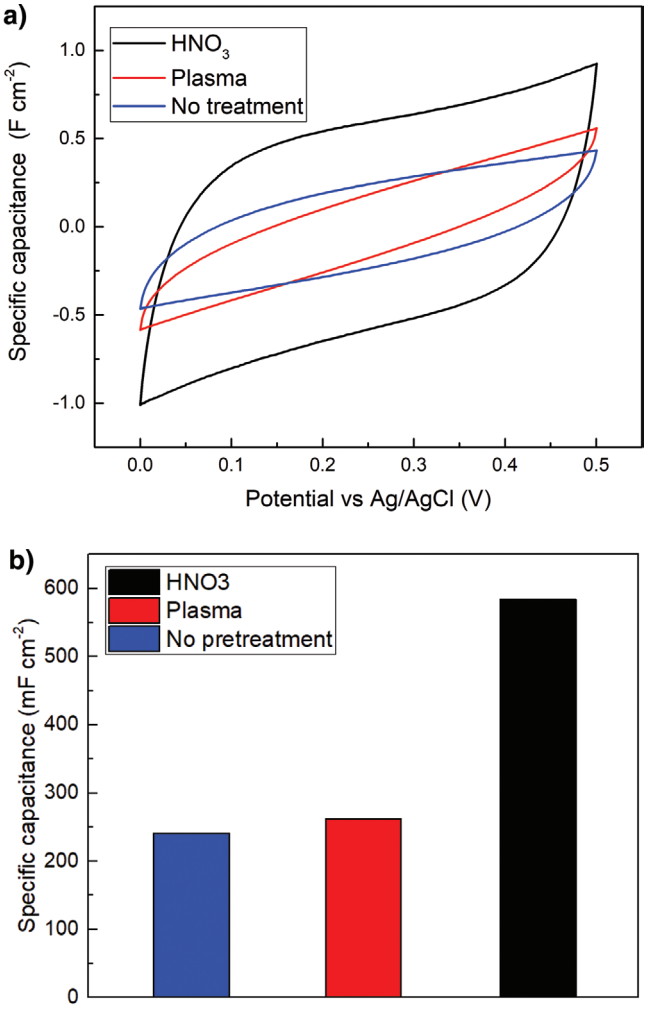

Figure 3. Comparison of HNO_3- and plasma-treated samples with pristine counterpart: a) CV performed in a three-electrode configuration and b) specific capacitance evaluated by three-electrode CV.

system (Q150T-ES, Quorum Technologies) at 10^{-4} bar, applying a 30 mA current for 120 s. Fourier transformed infrared (FTIR) and contact angle measurements were conducted to investigate the modification induced by the surface treatment of the LIG surface (see the Supporting Information). The HNO_3 incubation results in the formation of functional groups, while plasma does not modify the chemistry of the LIG surface (this is in line with the physical etching by Ar plasma). However, both the treatments are successful in the increase of the LIG wettability as demonstrated by the contact angle results (see Figure S8, Supporting Information).

The electrochemical measurements were then performed on samples decorated with AC deposited in vacuum, with the same parameters discussed above.

It is easy to appreciate from **Figure 3** that the treatment in nitric acid is much more effective than that with plasma toward performances increasing for AC-decorated LIG samples, while keeping a very high efficiency which implies that no redox reactions are taking place. However, we think that it could be very intriguing to deeply investigate in a further study the effect of plasma treatment on LIG surface tuning the dry etching parameters, such as power, time, and chemistry of the plasma.

In order to verify that the capacitance increase can be ascribed solely to the impregnation of the LIG electrode without increasing the available area, field emission scanning electron microscopy (FESEM) images were acquired confirming the absence of changes in LIG morphology and geometry (**Figure 4**a). Figure 4b,c shows images with higher magnifications for AC-impregnated LIG, while Figure 4d shows LIG before impregnation. The direct comparison between Figure 4c,d allows to observe the perfect compatibility between the LIG macropores and AC microparticles trapped into the LIG network. This is the reason of the huge improvement in capacitance, since LIG acts as a sort of 3D current collector, i.e., a sponge filled by the AC particles, guaranteeing their electrical interconnection.

After having identified the best optimization procedure to increase EDL capacitance, supercapacitors were fabricated and characterized in two-electrode configuration (see Figure S2, Supporting Information). The interdigitated μSCs were assembled in a flexible packaging, exploiting a glass fiber separator swollen into a water-based electrolyte. Contacts were fabricated laying titanium grid on the lower part of the device, then pouring a conductive carbon paste and pressing the grind onto the device. Finally, the device was enclosed in pouch through a vacuum sealer, overall leading to a flexible device able to avoid the evaporation of the electrolyte.

Figure 5 collects the electrochemical characterization of the fabricated device, before and after nitric acid treatment and AC infiltration. All the CV measurements recorded for composite-based devices showed a box-like shape, without peaks along all the curves. Even in device configuration, the capacitance rise induced by nitric acid functionalization was clearly evident, and the infiltration with AC further improved the overall performances. The optimized LIG-based μSC was able to reach 20.7 mF cm^{-2}, with an enhancement of about 42 times with respect to the bare LIG device. This value is the highest ever obtained for an LIG device exploiting only EDLC storage mechanism.

However, it is worth to notice that the specific capacitance values were lower in comparison with the data shown in Figure 3. Even if a certain difference in the calculated capacitance (usually toward lower values) between the three- and two-electrode configuration is quite commonly observable, the here presented data show a too marked variation to be only ascribed to this fact. We believe that this trend can be attributed to the geometry selected for the two measurements. Indeed, for 3-electrode measurements we designed a small circular area of LIG (≈600 µm in diameter), connected to an LIG line to take the contact to the working electrode (see Figure S3, Supporting Information). In order to minimize the contribution on the resistance of LIG on the capacitance analysis, we used a titanium foil pressed onto the LIG line near to the dot, but ensuring no contact with the electrolyte solution thanks to an elastomeric gasket. This configuration was selected in order to reach a deep understanding of the LIG performance when subjected to the different treatments. However, it is inevitably most favored by an electrical conductivity point of view with respect to the interdigitated device.

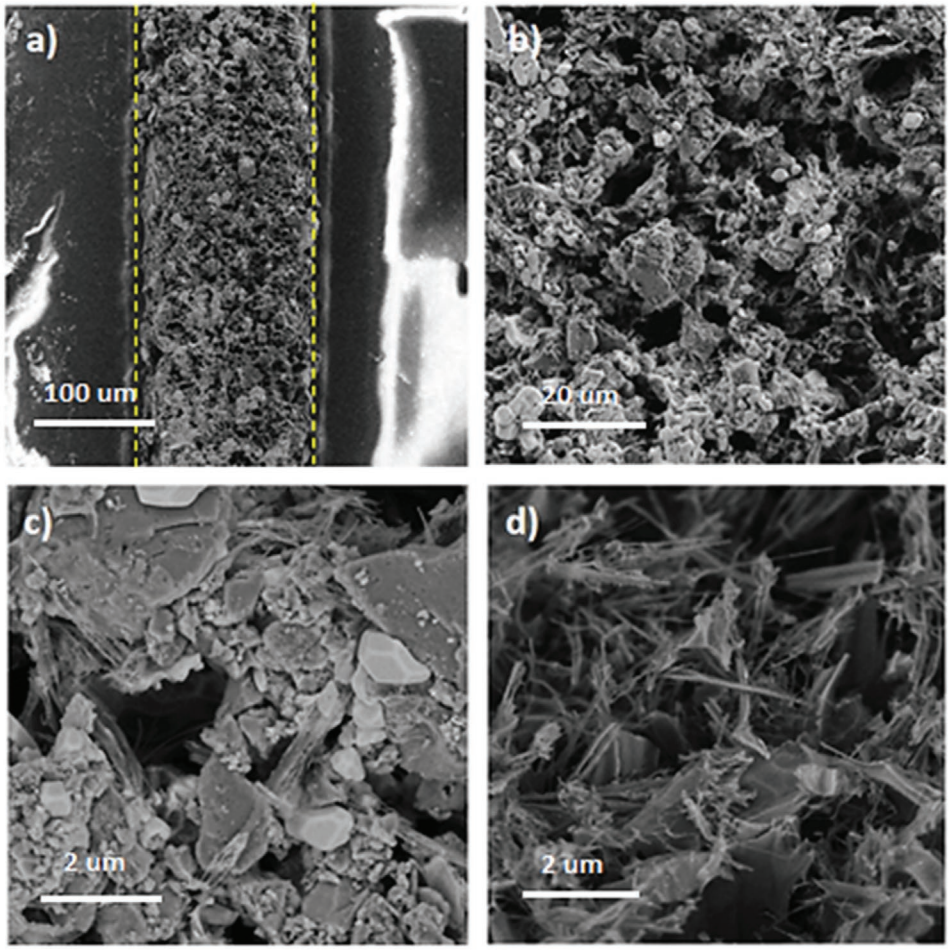

Figure 4. a–c) FESEM images under different magnifications for LIG electrode decorated with AC particles. Panel (d) shows the bare LIG electrode at high magnification as comparison.

Focusing on devices response, it is possible to state that the device treated with HNO_3 and infiltrated with the AC compound carried much higher capacitance with respect to the bare device (Figure 5a), reaching up to 20.7 mF cm^{-2} at a scan rate of 5 mV s^{-1} (Figure 5d).

The series resistance of the whole device is strongly reduced after the treatment, achieving about 100 Ω cm^{-2}. Electrochemical impedance spectroscopy (EIS) also showed that, before treatment, an inhomogeneous behavior of the electrode, highlighted by the semicircle in the red curve, was present. Usually, in the study of pseudocapacitive materials or other batteries, this semicircle can be ascribed to charge transfer resistance.[25] When speaking about pure EDLC working mechanism, assuming that there is not electron transfer at the interface, it was described as a contact resistance attributable to the presence of functional groups on the carbon-based material.[26]

Also in this case this hypothesis can be taken into account since, even if no pseudocapacitive materials were added on the working active material, the presence of a lot of functional groups on the LIG surface have been previously demonstrated.[27] However, after the immersion in HNO_3, this behavior was reduced and then completely disappeared when the AC particles were included into the 3D network.

The Coulombic efficiency of the device during the CV at scan rate 5 mV s^{-1} was overall high, i.e., on average above 98%. Coulombic efficiency was also investigated under different current ranges in galvanostatic measurements, at very low currents, the Coulombic efficiency was pretty low, around 86%, but raising the applied current up to 0.1 mA cm^{-2} pushed the efficiency up to 95.6%. The same trend was observed at even higher current density values, since these conditions let the device spend less time at the voltage boundaries, where irreversible reactions can damage the electrolyte itself.

Energy and power densities have also been derived, in order to retrieve a Ragone plot (Figure 5f). The device here studied showed fairly high power and energy compared to the current state of art for LIG.

Aging measurements were carried out performing a float test on different samples. The capacitance initially retained stabilized after ≈200 h to the 90% of the initial value. This value was then kept for other 420 h (**Figure 6**a) confirming the stability performance of the proposed device.

Finally, since one big advantage of these devices is the flexibility, electrochemical measurements were also carried out bending the device (Figure 6b) also at different angles, and then putting it to rest again (Figure 6c). CV traces show that, keeping the device

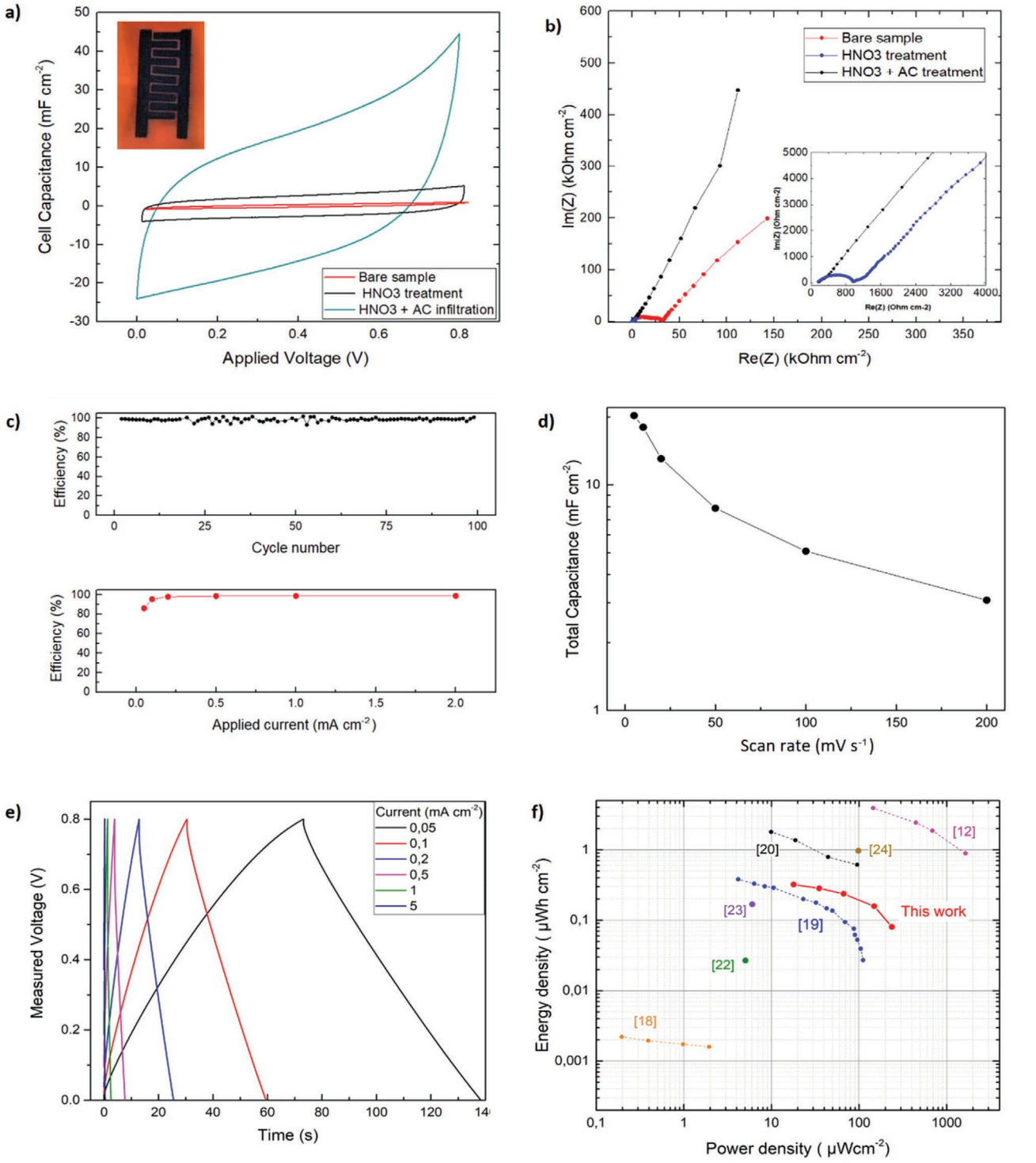

Figure 5. a) CVs (at 5 mV s^{-1}, electrolyte: KCl 1 M) of the bare device and after nitric acid treatment and AC infiltration. b) EIS spectra comparison between treated and untreated samples. c) Coulombic efficiency of the AC-treated device versus cycle number and applied currents. d) Specific capacitance of the treated device with respect to scan rates. e) Galvanostatic charge discharge of the treated device at different current ranges. f) Ragone plot compared with flexible LIG state of the art.[12,18–20,22–24]

curved, the decrease of capacitance is very small, and resting it again makes this value rise a bit, reaching the 90% of the initial capacitance. This is probably only due to the contact between the glass fiber and the supercapacitor, that is less adherent while keeping the device bended and possible variation in interconnection among the LIG flakes that deteriorates during bending.

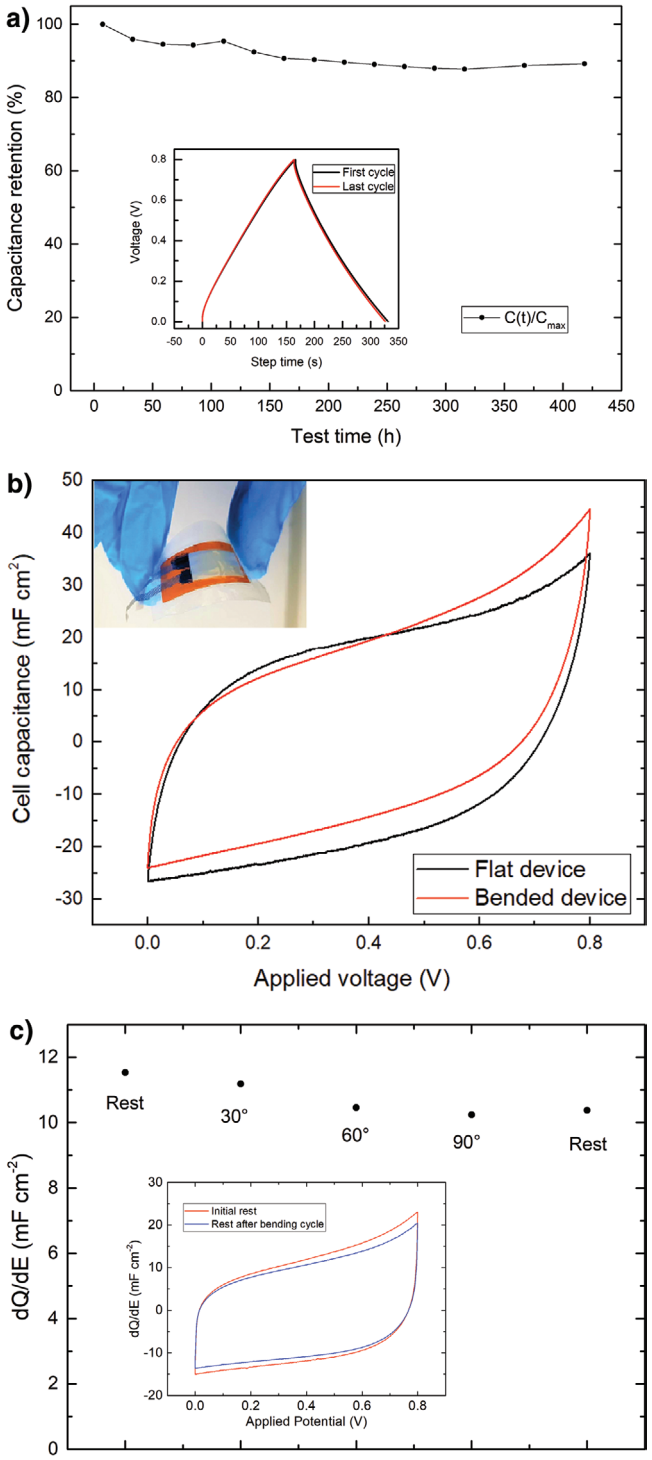

Figure 6. a) Float test: capacitance retention with respect to time. In the inset: Voltage shape in time at the first cycle and at the end of the measurement (after 420 h). b) Cyclic voltammetry of the flat and bended device. c) Capacitance retention at different bending angle and then the return flat condition.

3. Conclusions

In conclusion, this paper reports on the capacitance enhancement of LIG electrodes without exploiting pseudocapacitive materials. The proposed strategy relies on the infiltration of the graphene-based 3D network with porous AC particles. Several impregnation approaches were investigated, among which vacuum infiltration turned out to be the most effective. The perfect matching between the dimensions of LIG macropores and AC microparticles allowed an outstanding increase in terms for specific capacitance for the newly designed materials. Furthermore, LIG wettability was tuned by physical and chemical methods in order to improve AC infiltration. Wet chemical methods consisting of nitric acid incubation resulted to be the best choice to further boost the EDL capacitance rise.

Finally, μSC prototypes were assembled to demonstrate the effective applicability of the proposed approach to energy storage device fabrication, with an overall increase of more than one order of magnitude of the specific capacitance, retaining excellent Coulombic efficiency.

4. Experimental Section

LIG Device Fabrication: Initially, the LIG pins were fabricated with different set of laser parameters, as shown in the Supporting Information. The chosen set was the needle since it provided rather high capacitive and conductive structures. Laser writing was carried out on Dupont 125 μm polyimide sheets.

On the other hand, the LIG supercapacitors were fabricated exploiting a CO_2 laser source (EOX 30W laser by Datalogic, implemented in a Microla Optoelectronics laser writing system). This laser works with a Pulsed Width Modulation control of the laser source. The laser parameters were set as following, where * is the dot per inches:

Mode	Resolution	Frequency	Laser velocity	Laser power
Raster	400 dpi*	4000 Hz	375 mm s^{-1}	5.7 W

Raster is the writing mode: the laser writes in rows. The rows are written from left to right and from right to left alternatively. The other set of parameters affect the dose of energy sent to the device, and after several attempts this configuration has been discovered to one that provides the LIG lines with the lowest resistivity. Supercapacitors (see the Supporting Information) have ten pins, each one 4 mm long and 1 mm wide. The whole device results to be 1.2 × 1.5 cm^2.

Nitric Acid Treatment: The treatment to turn the LIG device into hydrophilic surface was carried out immerging it into a 60.5% concentrated HNO_3 solution. The device was kept in solution for 10–15 s, then it was rinsed with distilled water.

Electrodes Preparation: All the chemicals used in this work were purchased from Sigma-Aldrich and used as received, with the exception of the activated carbons and the C65 CB, acquired from MTI.

Activated carbons have a surface area of 1666 m^2 g^{-1}, a particle size of 10–30 μm and an ash content <1%.

The slurry was prepared employing DMSO as solvent, adding at first the binder agent, PVDF, and subsequently the CB and AC components.

5 mL of DMSO were used for each gram of active material, conductive and binder agents. LIG electrodes were left into the slurry for 30 s for dipping procedure and were then rinsed with DMSO in order to remove the nontrapped AC nanoparticles.

Vacuum procedure follows the dipping one, but applying low-vacuum to the solution (about 10 mbar) in a time range 30–300 s.

Characterization: Electron microscopy analysis was performed with an FESEM Supra 40 (Zeiss). Electrochemical characterizations were run with a VMP3 potentiostat (Biologic), using micromanipulators to contact the device.

FTIR spectra were recorded using a Nicolet 5700 FTIR spectrometer used in attenuated total reflectance mode with 2 cm^{-1} resolution and an average of 32 scans.

Static contact angle measurements were performed using optical contact angle H200 Dataphysics equipment in ambient conditions. The sessile drop method was implemented employing water droplets with 1.5 µL volume.

CV experiments were carried out in the potential window 0–0.8 V, while galvanostatic charge and discharge measurements were performed according to devices rate capabilities, spanning from 0.05 to 5 mA cm^{-2}. Finally, the ageing performance was carried out with the Arbin BT2000: the device was kept at 0.8 V for 3 h, followed by 50 cycles of charge discharge at 10 mA in the 0–0.8 V potential window.

LIG pins were contacted with a titanium grid and covered with polydimethylsiloxane (PDMS). A hole in the PDMS was fabricated, in order to connect the active area with a glass pipe filled with water-based electrolyte (1 M KCl), where the reference electrode and the counter electrode were immerged (see the Supporting Information).

On the other hand, the LIG supercapacitor was sealed in pouch (see the Supporting Information), therefore it just needed to be connected to the instrument terminals.

Supporting Information

Supporting Information is available from the Wiley Online Library or from the author.

Acknowledgements

This result is part of a project that has received funding from the European Research Council (ERC) under the European Union's ERC Starting Grant CO_2CAP Grant agreement No. 949916 (Energy harvesting from CO_2 emission exploiting ionic liquid-based CAPacitive mixing).

Open access funding provided by Politecnico di Torino within the CRUI-CARE Agreement.

Conflict of Interest

The authors declare no conflict of interest.

Data Availability Statement

Research data are not shared.

Keywords

activated carbon, EDLC, laser-induced graphene, LIG, supercapacitors

Received: August 7, 2021
Revised: October 6, 2021
Published online: November 7, 2021

[1] R. Ye, D. K. James, J. M. Tour, *Acc. Chem. Res.* **2018**, *51*, 1609.
[2] A. Lamberti, F. Clerici, M. Fontana, L. Scaltrito, *Adv. Energy Mater.* **2016**, *6*, 1600050.
[3] X. Wang, Q. Zhang, *J. Energy Storage* **2021**, *34*, 101994.
[4] W. Gao, N. Singh, L. Song, Z. Liu, A. L. M. Reddy, L. Ci, R. Vajtai, Q. Zhang, B. Wei, P. M. Ajayan, *Nat. Nanotechnol.* **2011**, *6*, 496.
[5] N. A. Kyeremateng, T. Brousse, D. Pech, *Nat. Nanotechnol.* **2017**, *12*, 7.
[6] J. Lin, Z. Peng, Y. Liu, F. Ruiz-Zepeda, R. Ye, E. L. G. Samuel, M. J. Yacaman, B. I. Yakobson, J. M. Tour, *Nat. Commun.* **2014**, *5*, 5714.
[7] A. Lamberti, F. Perrucci, M. Caprioli, M. Serrapede, M. Fontana, S. Bianco, S. Ferrero, E. Tresso, *Nanotechnology* **2017**, *28*, 174002.
[8] L. X. Duy, Z. Peng, Y. Li, J. Zhang, Y. Ji, J. M. Tour, *Carbon* **2018**, *126*, 472.
[9] Z. Peng, R. Ye, J. A. Mann, D. Zakhidov, Y. Li, P. R. Smalley, J. Lin, J. M. Tour, *ACS Nano* **2015**, *9*, 5868.
[10] W. Song, J. Zhu, B. Gan, S. Zhao, H. Wang, C. Li, J. Wang, *Small* **2018**, *14*, 1702249.
[11] L. Li, J. Zhang, Z. Peng, Y. Li, C. Gao, Y. Ji, R. Ye, N. D. Kim, Q. Zhong, Y. Yang, H. Fei, G. Ruan, J. M. Tour, *Adv. Mater.* **2016**, *28*, 838.
[12] F. Clerici, M. Fontana, S. Bianco, M. Serrapede, F. Perrucci, S. Ferrero, E. Tresso, A. Lamberti, *ACS Appl. Mater. Interfaces* **2016**, *8*, 10459.
[13] C. Zhang, Z. Peng, C. Huang, B. Zhang, C. Xing, H. Chen, H. Cheng, J. Wang, S. Tang, *Nano Energy* **2021**, *81*, 105609.
[14] E. Aparicio-Martínez, A. Ibarra, I. A. Estrada-Moreno, V. Osuna, R. B. Dominguez, *Sens. Actuators, B* **2019**, *301*, 127101.
[15] S. Nasraoui, A. Al-Hamry, P. R. Teixeira, S. Ameur, L. G. Paterno, M. Ben Ali, O. Kanoun, *J. Electroanal. Chem.* **2021**, *880*, 114893.
[16] A. Chhetry, M. Sharifuzzaman, H. Yoon, S. Sharma, X. Xuan, J. Y. Park, *ACS Appl. Mater. Interfaces* **2019**, *11*, 22531.
[17] Y. Zhang, N. Li, Y. Xiang, D. Wang, P. Zhang, Y. Wang, S. Lu, R. Xu, J. Zhao, *Carbon* **2020**, *156*, 506.
[18] M. Parmeggiani, P. Zaccagnini, S. Stassi, M. Fontana, S. Bianco, C. Nicosia, C. F. Pirri, A. Lamberti, *ACS Appl.Mater. Interfaces* **2019**, *11*, 33221.
[19] A. Lamberti, M. Serrapede, G. Ferraro, M. Fontana, F. Perrucci, S. Bianco, A. Chiolerio, S. Bocchini, *2D Mater.* **2017**, *4*, 035012.
[20] P. Zaccagnini, D. di Giovanni, M. G. Gomez, S. Passerini, A. Varzi, A. Lamberti, *Electrochim. Acta* **2020**, *357*, https://doi.org/10.1016/j.electacta.2020.136838.
[21] Y. Lu, H. Lyu, A. G. Richardson, T. H. Lucas, D. Kuzum, *Sci. Rep.* **2016**, *6*, 33526.
[22] J. Bae, M. K. Song, Y. J. Park, J. M. Kim, M. Liu, Z. L. Wang, *Angew. Chem., Int. Ed.* **2011**, *50*, 1683.
[23] Y. Meng, Y. Zhao, C. Hu, H. Cheng, Y. Hu, Z. Zhang, G. Shi, L. Qu, *Adv. Mater.* **2013**, *25*, 2326.
[24] Y. Fu, H. Wu, S. Ye, X. Cai, X. Yu, S. Hou, H. Kafafy, D. Zou, *Energy Environ. Sci.* **2013**, *6*, 805.
[25] D. Takamatsu, Y. Koyama, Y. Orikasa, S. Mori, T. Nakatsutsumi, T. Hirano, H. Tanida, H. Arai, Y. Uchimoto, Z. Ogumi, *Angew. Chem., Int. Ed.* **2012**, *51*, 11597.
[26] Y. R. Nian, H. Teng, *J. Electroanal. Chem.* **2003**, *540*, 119.
[27] M. d'Amora, A. Lamberti, M. Fontana, S. Giordani, *J. Phys.: Mater.* **2020**, *3*, 034008.